international journal of

powder metallurgy

Summer 2021

57/3

PM Design Excellence Award Winners

State of the PM Industry in North America—2021

A Comparison of the Spreadability and Flowability of Metal Powders for AM Applications

A COMPARISON OF THE SPREADABILITY AND FLOWABILITY OF METAL POWDERS FOR AM APPLICATIONS

Greg Martiska*

The spreadability and flowability of three sets of metal powders manufactured for additive manufacturing (AM) applications have been measured for a range of layer thicknesses under different application conditions including a range of spreading speeds, different spreader geometries, a range of powder feeding geometries, spreader application pressures, and different environmental conditions. Spreadability measurements were made using a spreadability analyzer. Spreadability data presented include spreading efficiency, mass per spreader travel, and spreading uniformity per spreader travel. Flowability measurements were made using a rotating drum rheology tester. Flowability data presented include avalanche energy, avalanche angle, and dynamic density. Samples were tested as received and were subsequently exposed to humidity, drying, and segregation stress.

INTRODUCTION

The ability of a powder to form a consistent layer in an additive manufacturing (AM) machine is critical to producing high quality parts. This ability is referred to as powder spreadability. There are many official and unofficial definitions of powder spreadability but there is no consensus on how to test it. Many machines have various in situ techniques for analyzing powder layer formation, but these techniques are more for process monitoring than predictive testing. Several tests and test devices have been proposed.[1–4] These include test beds that automatically spread a test powder, and manual spreading devices. Typically the measurement performed is an optical analysis of the top surface of the powder layer. In some cases, the density of the layer is measured by weighing the powder and calculating the spread layer volume.

In lieu of spreadability tests researchers and parts makers have relied on powder flow measurements to predict and study spreadability. Powder flow measurements generally study the interactions of powder particles in a powder bed and these measurements are referred to as powder flow properties. The flow properties are then correlated to performance on the AM machine. The problem with this approach is that flowability and flow properties are not the only variables that affect spreadability. Machine variables and other powder variables as listed in Table 1 are equally or more important.

To address this problem a new device has been introduced commercially to measure powder spreadability. The SpreadStation Powder Spreadability Analyzer (subsequently referred to as a spreadability analyzer (Figure 1a)) creates up to four simultaneous layers of powder using various spreader geometries, spreader speeds, and powder feeding options. The analyzer then measures the quality of the powder layer using optical techniques and by measuring the mass of material exiting the spreader. The test powder can be spread on various build plates or on a powder bed.

For a powder to form a layer on a build plate there must be relative motion between the spreading device and the build plate. In most AM machines the spreading device moves over the build plate to spread the powder. In the spreadability analyzer, the build plate is moved under the spreading device to spread the powder. The build plate is rotated relative to the spreading device to keep the system small, to control environmental conditions, and to provide

*Technical Manager, Mercury Scientific Inc., 64 Barnabas Drive Unit 1, Newtown, Connecticut 06470; USA; Email: greg@mercsci.com

TABLE I: VARIABLES IN AM APPLICATIONS

Printing Variables	Material Variables
Leveling Height	Particle Size and Distribution
Spreader Speed	Flowability
Spreader Geometry	Particle Shape
Pressure on the Powder	Surface and Moisture Properties
Powder Feeding System	Static Charge
Environmental Conditions in the printer	Segregation

unlimited travel for the build plate (Figure 1b). This simplifies the design of the device and makes it easier to mount measuring systems as they are stationary. After being spread, the powder is removed from the build plate by an angled scraping blade (Figure 1b) and transferred to a balance to be weighed. The instrument can be equipped with multiple spreaders and balances.

The spreading assembly (Figure 2) for the analyzer consists of three parts: 1) a spreading base, 2) a spreading plate, and 3) a powder feeder (Figure 3). The spreading plate is mounted on the spreading base and can move in the vertical direction to create a gap between the build plate and the spreading plate to allow powder spread. The spreading device moves up and down with any unevenness in the build plate to maintain a constant spreading gap. Many spreading geometries are available including flat-edged, round-edged, flexible, and counter rotating cylinder. The spreading base maintains the powder behind the spreading plate. The powder feeder delivers the powder to the spreading area. The angle and gap of the feeder can be adjusted as well as the pressure on the powder in the spreading area. Up to four spreading devices can be mounted on the analyzer to spread four layers simultaneously. When the test powder has been loaded in the powder feeder, the movement of the build plate is started, and the powder is spread in a layer on the build plate where it is subsequently measured.

Several measurements are made to assess the powder layer. The primary measurement is the mass of powder that exits the spreader relative to the motion of the build plate. After exiting the spreading device, the powder is moved off the build plate and onto a balance by an angled scraping blade. The balance measures the mass of powder removed from the build plate over time. Before reaching the blade, images of the powder are taken, and the thickness of the powder bed is measured using a distance sensor. The density of the bed is calculated from the height of the powder or spreading gap and the travel of the build plate. Channels and waves in the powder layer are detected using image analysis techniques on the powder images.

These measurements allow the layer uniformity and density to be measured over the course of the spreading until no more powder exits the spreading device. The spreading efficiency is the spreading density of the layer relative to a layer of solid powder material at the thickness of the spreading gap. The spreading rate is the mass of powder in the layer per centimetre traveled by the build plate. The standard deviation of the spreading rate is the standard deviation of the mass of powder being spread taken every second. The spread uniformity compares the spreading rate at the beginning of the measurement and at the end of the measurement with the average spread rate. A uniformity of zero means there is no variation in the spreading rate. A negative uniformity means less powder is being spread at the end of the test compared with the beginning. A positive uniformity means more powder is being spread at the end of the test than at the beginning. The fractal dimension is the smoothness of the mass in the spread layer.

To compare the spreadability of a powder with its flowability, the flow properties of the powders were characterized with a rotating drum rheology tester that is very sensitive to small changes in AM powders. The

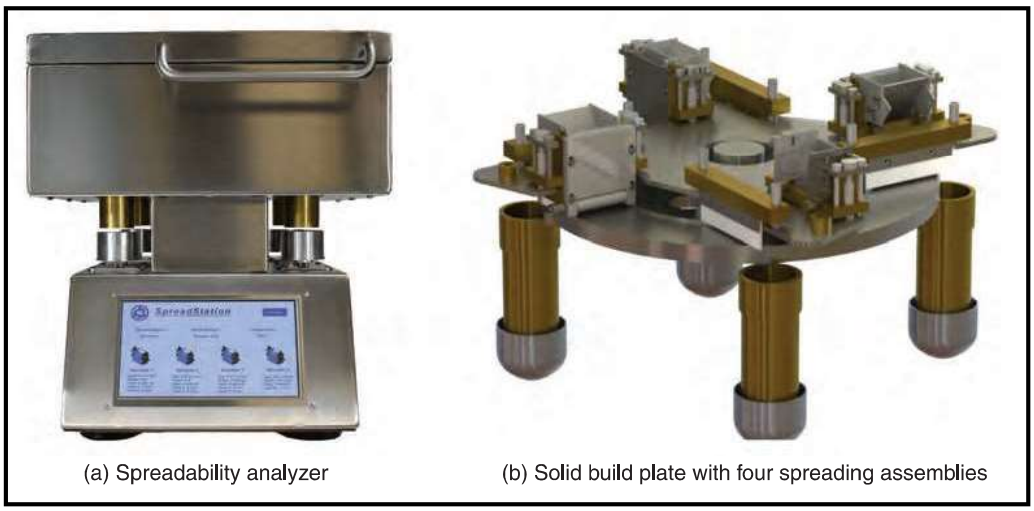

(a) Spreadability analyzer (b) Solid build plate with four spreading assemblies

Figure 1. *Spreadability analyzer*

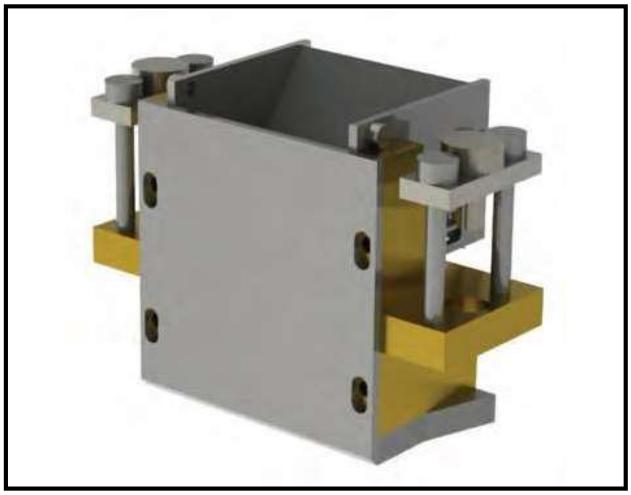

Figure 2. *Spreading assembly with spreading base, spreading plate and powder feeder installed*

Figure 3. *Powder feeder*

analyzer has demonstrated the capability to capture differences in 316L stainless steel powders atomized by argon or nitrogen.[5] The argon atomized powder consistently displayed better flowability than the nitrogen atomized powders measured by a flow test using the analyzer. These differences in flowability were correlated to the powder morphology, with argon atomized powder displaying higher sphericity. Differences in flowability of virgin and recycled 304L stainless steel powders were also identified using the rotating drum tool.[6] After 7 uses, both the particle-size-distribution (PSD) and particle shape changed, which resulted in the different flow properties of the recycled powder. Elemental iron and nickel powders were also tested using the analyzer with respect to their flow properties.[3] With different PSD and particle shape, the powders displayed different flow properties that were successfully captured by the rotating drum device.

This paper is a companion paper to prior publications[7,8] that contain the full details of the spreadability and flowability measurements of the samples.

Materials

Two different groups of 316L austenitic stainless steel powder samples were tested. They are labeled Samples A and B. Each group consisted of a virgin sample and a recycled version of the same material. For the A samples, the recycled material had been through just two machine cycles. For the B samples, the recycled material had been through eight machine cycles. These materials have been characterized extensively previously.[9,10]

An additional group of nickel alloy powders was also tested that consisted of both virgin and recycled material. These samples were labeled C. The virgin material was reported to be acceptable and the recycled material unacceptable for an AM build application.

EXPERIMENTAL

The flowability of the samples was tested using a rotating drum rheology tester that utilizes a rotating drum with transparent sides. During the tests, a powder volume of 25 cm^3 or 100 cm^3 was loaded into the drum. As the drum was rotated on a pair of motor-driven rollers at pre-defined rotation rates, the avalanche profile of the powders was captured using a digital camera, with the assistance of cold-cathode back-light illumination, as shown in Figure 4. The images of the avalanche profile, taken at 20 frames per second, were collected and processed to capture the exact motion of the powder samples. Image analysis was conducted on the images collected, and numerous parameters were measured or calculated. A reference mask allows calibration of the imaging system. Several testing modes are available on the drum analyzer that include flow, packing, multi-flow, and static charging tests.[11] Each test examines a unique aspect of powder properties. In this case the powders were tested with the flow test.

In the flow test, a relatively low rotation rate of 0.3 rotations per minute (rpm) is used, and the details of the avalanche behaviors are captured. The instrument captures 100 avalanches and provides averaged results. Flow properties of the powder can be evaluated by measuring the avalanche angles, which are captured by the camera when a powder avalanche begins. The break energy represents the maximum potential energy level of the powder test portion before an avalanche begins. The avalanche energy is the amount of energy released during an avalanche. The dynamic density can be calculated from the measured mass of the powder and the bulk volume, determined using image analysis tools as the drum is rotating. The cohesion-T is the average of the shear stress overcome by the flowing layer as the powder moves during an avalanche.

Figure 4. *Illustration of working principle of rotating drum analyzer. Avalanche profile of powders is captured by a camera as the drum is rotating. The avalanche angle α is measured by image analysis.*

Measurements of powder spreadability were made using the spreadability analyzer. The analyzer was equipped with flat-edged and round-edged spreading plates with spreading gaps from 50 µm to 200 µm. Powders were tested at spreader speeds from 50 mm/s to 200 mm/s. The analyzer was equipped with a machine-vision camera and LED lighting to capture images of the spread powders, and a laser triangulation distance sensor to measure spread-layer thickness.

The low-pressure powder feeder used had a feed angle of 60° and a feeding gap of 4.6 mm. The high-pressure feeder consisted of a rectangular opening with a mass on the powder to change the pressure on the powder in the spreading area. The build plate consisted of a stainless-steel disc. The effect of flat-edged and round-edged spreading plates was evaluated.

For each test, 40 g or roughly 10 cm^3 of sample was tested. Test time was 30 s to 50 s from the start of spreading to the end of spreading and the total travel of the spreading assemblies was 200 to 300 cm, which is equivalent to a 2- to 3-metre-long build plate.

Spreader bases and powder feeders were removed and wiped with a dry towel to clean them between samples. The build plate was rotated for 200 cm at 50 mm/s to clean it prior to the next test. This required 33 seconds.

All samples were tested in the as-received condition. Some samples were then exposed to humidity by placing them in an open pan in an oven with a relative humidity of 40% and a temperature of 50 °C for two hours, with mixing every 30 minutes to expose additional surfaces to the oven humidity. These samples were then cooled to room temperature and tested. After testing, these samples were dried at 100 °C for 16 hours, and then at 200 °C for two hours with mixing every 30 minutes. Samples were then cooled and tested again.

Some samples were also exposed to segregation stress. Test portions (75 cm^3) of various A and B samples were poured in turn through a closed-core flow funnel. A closed-core flow funnel has a shallow angle so that the powder flows in a first in last out pattern. When the funnel was opened the powder flowed into a second closed-core flow funnel. When the second funnel was opened the powder flowed into a third closed-core flow funnel. When the third funnel was opened, the first 25 cm^3 of powder exiting the funnel was collected and tested. Various A and B samples were also exposed to segregation stress using a pan sifting method. 100 cm^3 of each sample was transferred to a flat pan. The pan was shaken from side to side for 60 seconds to create motion in the sample. The top half of the sample was then scraped from the powder bed and collected. Then the lower layer was collected. Each pan layer was then tested.

RESULTS AND DISCUSSION

The spread layer thicknesses used in this study were selected to match the effective layer thickness of the powder layers in a typical powder-bed-fusion system. This effective layer thickness has been measured to be five to ten times the leveling height of the build platform.[12,13] For a typical 20 or 30 µm leveling height the effective layer thickness over the printed parts is 100 to 200 µm.[12,13] The leveling height on a PBF-LB unit is the amount of vertical movement of the spreader for each layer and is typically a constant value. The gap between the spreader and the part surface is not constant and depends on the thickness of the melt pool of the material and the thickness of the previous layer of powder. A feedback loop exists between the spreading gap and the actual thickness of the current and previous powder layer. If the current layer is thinner than the previous layer, then the next layer will have a larger spreading gap which in turn should create a thicker powder layer. If the current layer is thicker than the previous layer, then the spreading gap will be smaller for the next layer. This is also true for the density of the powder layer. A denser layer will form a thicker melt pool which will create a smaller spreading gap for the next layer and vice versa.

The effective layer thickness is also influenced by the

TABLE II. SUMMARY OF THE FLOWABILITY DATA FOR VARIOUS A, B, AND C AS-RECEIVED SAMPLES RANKED BY AVALANCHE ANGLE

Sample (as-received)	Avalanche Energy mJ/kg	Avalanche Angle deg	Cohesion-T Pa	Dynamic Density g/cm^3	Volume Fraction
A Virgin	9.8	30.5	29.0	4.60	0.574
C Virgin	14.7	41.5	80.7	4.30	0.551
A Recycled	17.7	36.5	90.6	4.23	0.529
B Recycled	16.2	44.3	83.7	4.24	0.529
C Recycled	24.9	50.9	194.5	3.82	0.489
B Virgin	28.3	58.0	151.0	4.09	0.508

TABLE III. RANKING SPREADABILITY OF AS-RECEIVED SAMPLES TESTED WITH A FLAT-EDGED SPREADING PLATE, A SPREADING GAP OF 150 µm AND A SPREADING RATE OF 50 mm/s

Sample (as-received)	Spread Eff. %	Layer Density g/cm^3	Spread Rate mg/cm	Spread Rate SD mg/cm	Spread Unif. %	Fractal Dim.
A Recycled	51.1	4.09	213	21	14.3	2.67
B Recycled	49.3	3.94	207	14	9.0	3.38
A Virgin	47.0	3.76	197	7	-0.2	2.8
B Virgin	43.9	3.51	182	15	4.9	3.06
C Virgin	43.4	3.47	182	9	-1.8	3.16
C Recycled	28.6	2.45	130	10	3.6	5.00

size and size distribution of the powder particles, the shape of the powder particles, the flowability of the powder, the static charge on the particles, etc. For example, a 50 µm particle cannot move through a gap less than 50 µm. Powder particles also do not form a monolayer of particles in a powder layer. Therefore, the true layer thickness of powder particles over a part or powder bed will be larger than the leveling height of the printer and will be affected by the powder and machine properties.

For the flow measurements, a low drum speed has been used for two reasons. One is that the speed of the particles in the powder bed in the spreading area of typical devices has been observed to be low for many printers. The other reason is that low-speed tests are more sensitive to small changes in the powder that is being tested (based on 20 years of experience with the instrument). Low-speed tests emphasize particle-to-particle interactions in the powder as opposed to higher speeds that are more about the dilation of the powder bed due to higher particle velocities and aeration of the powder.

Spreadability and Flow of As-Received Samples

A summary of the flow measurements made on the individual as-received samples is given in Table II. These measurements included the avalanche energy, avalanche angle, and the cohesion-T values describing the shear properties of the powder layers during the avalanche. Generally, lower values for each of these metrics are considered indicative of better powder flow properties.[2,3] The dynamic density and volume fraction of the powder, which capture the packing density of the powder as the drum was rotated, were also measured. Unlike the other properties, an increase in dynamic density can be correlated with better flow properties.

A summary of the spreadability data for the samples when using a flat-edged spreading plate, a spreading gap height of 150 µm and a spreading speed of 50 mm/s is given in Table III. The results indicate that the virgin A sample had the best flow properties of the samples with the lowest avalanche energy, avalanche angle, and cohesion-T. However, the recycled A and B samples had better spreadability. The virgin B sample had the poorest flowability but not the poorest spreadability. The recycled C sample had the poorest spreadability. In an actual PBF machine, the virgin B sample performed acceptably while the recycled C sample did not perform well. In general, the flow data and the spreadability data correlate. The poorest flowing samples also have the poorest spreadability. However, the best flowing samples rank differently for spreading. The spreadability settings in this case would be the most forgiving as the spreading speed is low and the spreading gap is on the higher side.

The spreadability of the A samples for gaps of less than 150 µm is presented in Table IV. With a 100 µm spreading gap the virgin and recycled samples spread the same but when the gap was reduced to 50 µm the recycled material spread worse than the virgin sample. In this case, improving the flowability of the powder improves the spreadability as the spreading layer thickness is reduced.

The spreadability of the A samples for a gap greater than 150 µm is presented in Table V. With a 200 µm spreading gap the recycled material spreads better than the virgin sample. In this case improving the flowability of the powder worsens the spreadability as the spreading layer thickness is increased.

The spreading data with different spreading gaps

TABLE IV. SUMMARY OF THE SPREADABILITY DATA FOR AS-RECEIVED A SAMPLES WITH A FLAT-EDGED SPREADING PLATE, SPREADING SPEED OF 50 mm/s, AND SPREADING GAPS OF 50 µm AND 100 µm

Sample	Spread Eff. %	Layer Density g/cm^3	Spread Rate mg/cm	Spread Rate SD mg/cm	Spread Unif. %	Fractal Dim.
A Virgin - 50 µm gap	48.0	3.84	66	7	1.2	5.27
A Virgin - 100 µm gap	48.2	3.86	134	10	6.1	3.02
A Recycled - 50 µm gap	42.8	3.42	60	8	-16.3	5.63
A Recycled - 100 µm gap	48.3	3.86	136	9	-8.4	2.75

TABLE V. SUMMARY OF THE SPREADABILITY DATA FOR AS-RECEIVED A SAMPLES WITH A FLAT-EDGED SPREADING PLATE, SPREADING SPEED OF 50 mm/s, AND SPREADING GAP OF 200 µm

Sample	Spread Eff. %	Layer Density g/cm^3	Spread Rate mg/cm	Spread Rate SD mg/cm	Spread Unif. %	Fractal Dim.
A Virgin - 200 µm gap	52.9	4.24	297	10	1.7	2.80
A Recycled - 200 µm gap	56.7	4.54	318	11	2.6	2.39

suggest that a powder that has better flow will spread better with a smaller spreading gap, and a powder with slightly poorer flow will spread better with a larger gap. On an AM machine, the spreading gap is a function of the effective layer thickness, which is a function of the powder and machine properties.

The spreadability of the A samples for a gap of 150 µm and various speeds is presented in Table VI and Table VII. As the spreading speed is increased, the flowability of the powder sample has a negative effect on spreadability. The virgin A sample has better flowability than the recycled A sample yet has a lower spreading efficiency as spreading speed is increased from 50 mm/s to 200 mm/s. This could be because powders are moved through the spreading gap by shear forces transmitted through the powder from the relative motion between the spreader and the powder bed. Powders that flow better can transmit less shear force. The particles in powders that flow well can move around each other more easily due to pressure from the spreading blade. This is indicated by the fact that the height of layers for the virgin A samples is lower than the height

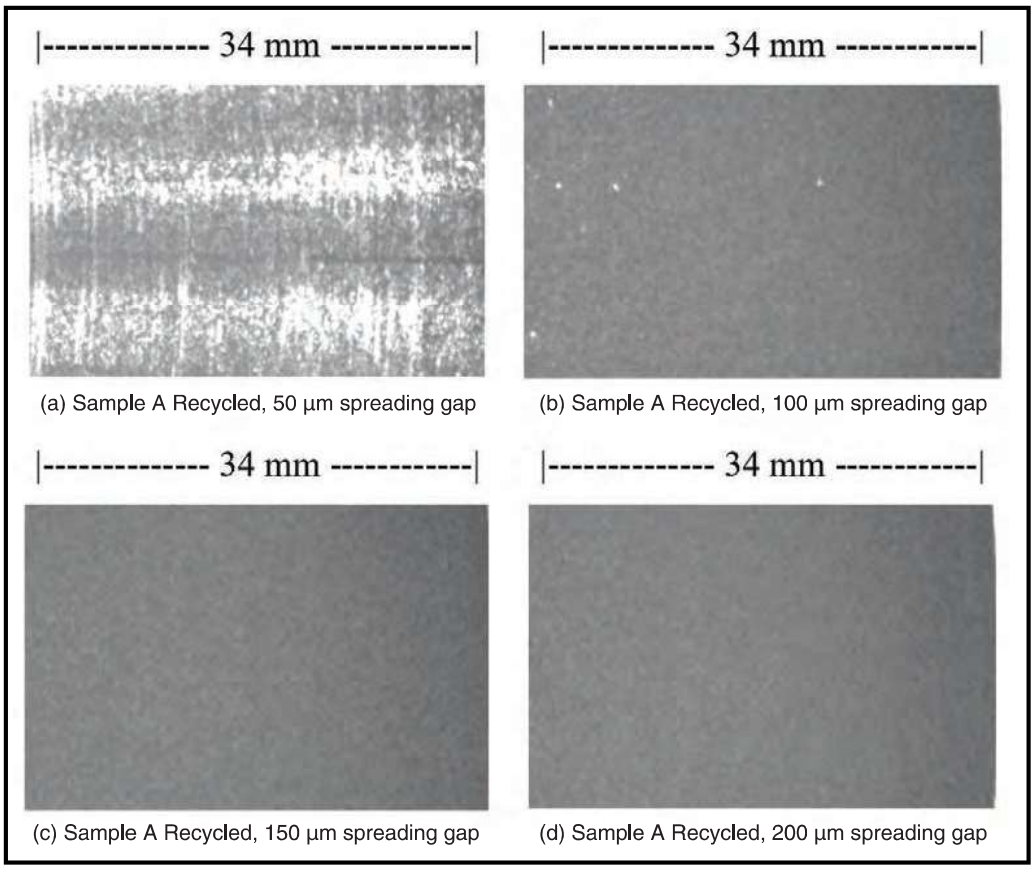

Figure 5. *Images of recycled A samples tested with a flat-edged spreading plate, spreading speed of 50 mm/s, and multiple spreader gaps*

TABLE VI. SUMMARY OF THE SPREADABILITY DATA FOR VARIOUS AS-RECEIVED SAMPLES WITH A FLAT-EDGED SPREADING PLATE, A 150 µm SPREADER GAP, AND MULTIPLE SPEEDS

Sample	Spread Eff. %	Layer Density g/cm^3	Spread Rate mg/cm	Spread Rate SD mg/cm	Spread Unif. %	Fractal Dim.
A Virgin, 50 mm/s	49.3	3.95	206	8	0.8	3.07
A Virgin, 100 mm/s	38.3	3.06	157	5	17.5	4.22
A Virgin, 150 mm/s	31.4	2.51	129	9	6.2	5.16
A Virgin, 200 mm/s	22.8	1.83	94	6	5.7	7.01
A Recycled, 50 mm/s	49.8	3.99	208	11	-7.7	2.76
A Recycled, 100 mm/s	42.3	3.39	178	10	-5.0	3.64
A Recycled, 150 mm/s	33.3	2.66	141	10	-18.4	4.58
A Recycled, 200 mm/s	31.9	2.71	217	11	-18.9	6.23
C Virgin, 50 mm/s	43.4	3.47	182	9	-1.8	3.16
C Virgin, 100 mm/s	38.3	3.29	174	8	2.1	3.51
C Virgin, 150 mm/s	29.4	2.52	134	9	-5.5	4.88
C Recycled, 50 mm/s	28.6	2.45	130	10	3.6	5.00
C Recycled, 100 mm/s	21.5	1.85	97	5	1.4	6.29
C Recycled, 150 mm/s	15.2	1.30	69	6	-2.3	8.03

TABLE VII. SUMMARY OF THE MEASURED LAYER THICKNESS FOR VARIOUS AS-RECEIVED SAMPLES WITH A FLAT-EDGED SPREADING PLATE, A 150 µm SPREADER GAP, AND MULTIPLE SPREADER SPEEDS

Sample	Measured Layer Thickness µm	Measured Layer Density g/cm^3	Measured Spread Efficiency %
A Virgin, 50 mm/s	158	3.75	46.9
A Virgin, 100 mm/s	117	3.92	48.9
A Virgin, 150 mm/s	100	3.78	47.2
A Virgin, 200 mm/s	72	3.82	47.8
A Recycled, 50 mm/s	171	3.49	43.7
A Recycled, 100 mm/s	135	3.77	47.1
A Recycled, 150 mm/s	106	3.76	47.0
A Recycled, 200 mm/s	88	3.68	45.9
C Virgin, 50 mm/s	132	3.94	45.9
C Virgin, 100 mm/s	118	4.18	48.6
C Virgin, 150 mm/s	86	4.43	51.5
C Recycled, 50 mm/s	73	5.02	58.4
C Recycled, 100 mm/s	72	3.87	45.0
C Recycled, 150 mm/s	15	—	—

of the layers for the recycled A samples. Interestingly, the layer density is slightly higher for the virgin A samples even though the layer height is lower.

The thickness of the spread layer decreases below the spreading gap height at speeds above 50 mm/s. This reduces the spreading efficiency calculated from the spreading gap height as the powder layer is no longer being spread at the gap height. However, the measured layer density remains relatively constant across all the spreading speeds except for the recycled C samples. The powder layer that is spread has a consistent density with increasing speed even though the thickness of the layer is decreasing as the spreading speed increases. The implication of this is that Sample A powders will spread uniformly at faster spreading speeds, but the melt pool thickness will decrease with increased speed. The recycled A sample material has slightly better spreadability under the conditions tested but its uniformity decreases with bed travel. This indicates that the recycled material is more affected by vertical pressure in the spreading zone compared with the virgin material.

The data for the C samples show similar speed sensitivity to that for the A samples. The difference between the two sample sets is that the A samples were acceptable for their AM application while for the C samples the recycled material was unacceptable. The test data indicated a clear difference between the spreadability of the virgin and recycled material with the recycled material having roughly half the spreading efficiency and spreading rate of the virgin material.

Images of the spread layer for the A samples (data in Table V) are presented in Figure 6. From the images, it can be observed that the powder layer becomes thinner and less uniform as the spreader speed increases. Thinner layers would affect all the parts in a build cycle while uniformity issues would potentially affect only certain parts in the build.

Images of the spread layer for the C samples (data in Table VIII) are presented in Figure 7. From the images, it can be observed that the powder layer becomes thinner and less uniform as the spreader speed increases.

Spreadability with a Round-Edged Spreading Plate

A summary of the spreadability ranking for as-received Samples A and B with a round-edged spreading plate, a spreading gap height of 150 µm, and spreading speeds of 50 mm/s is given in Table VIII. The round-edged spreading plate showed an increase in spreading efficiency for the A samples but little change for the B samples compared with the flat-edged spreading plate data in Table XI. The virgin A sample had better flow than the recycled A sample, but both had equal spreadability with the round-edged plate.

Spreadability and Flow of Humidity Exposed Samples

The flowability and spreadability of the humidity exposed A and B samples with a gap of 150 µm are presented in Table IX and Table X respectively. When the samples were exposed to humidity the flowability and spreadability rankings changed. Sample A virgin had the best flowability and spreadability. Sample B virgin had the poorest flowability and stopped spreading. What

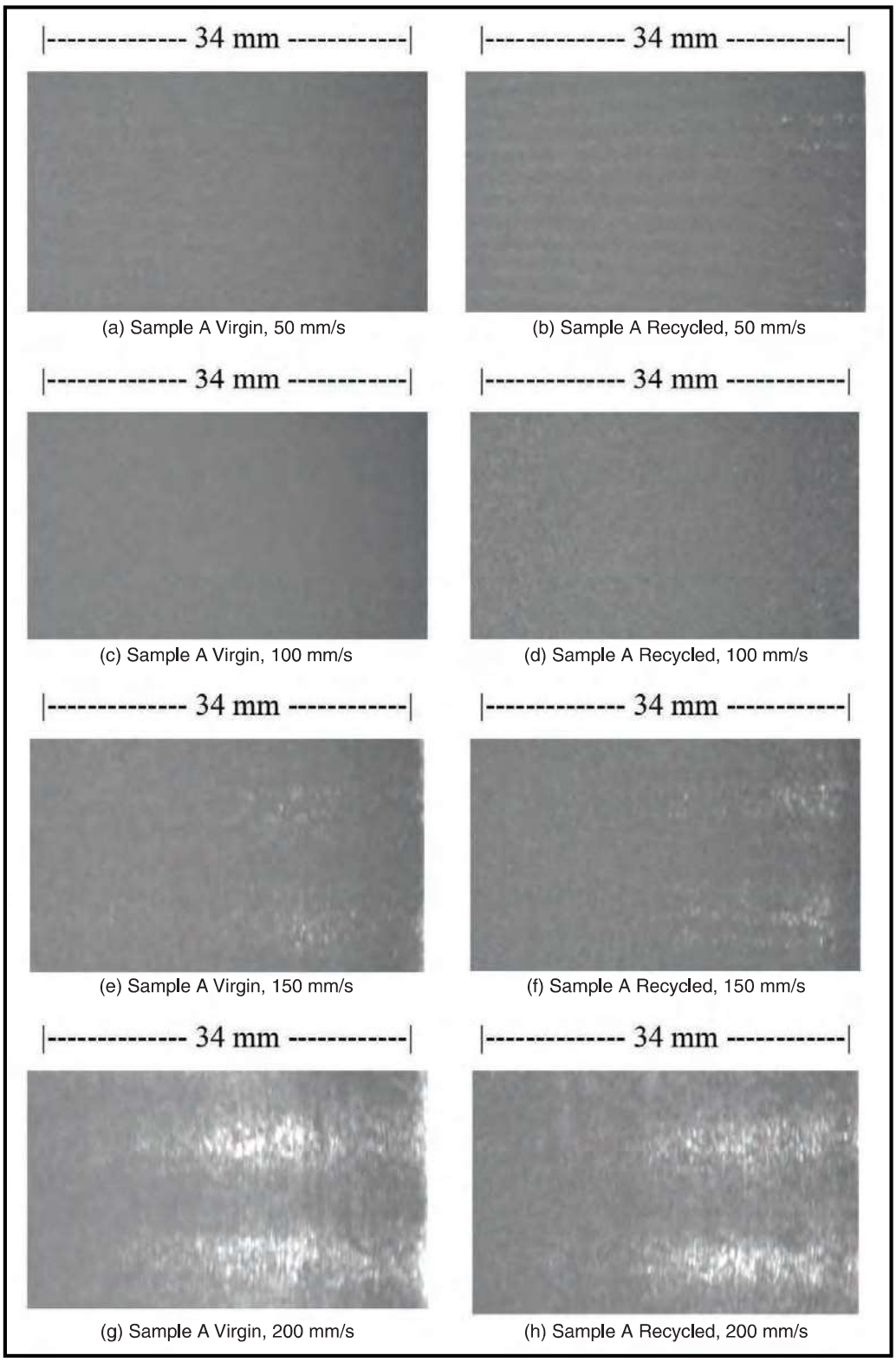

Figure 6. *Images of various as-received A samples tested with a flat-edged spreading plate, a 150 µm spreader gap, and multiple spreader speeds*

is interesting about the virgin B sample data is that exposure to humidity did not change the flowability of the sample to a large extent but completely stopped the powder from spreading. The virgin B sample exposed to humidity did have poorer flow than the as-received sample, but the difference was not as large as would be expected from the spreadability data. This indicates that exposure to humidity pushed the powder past a limit

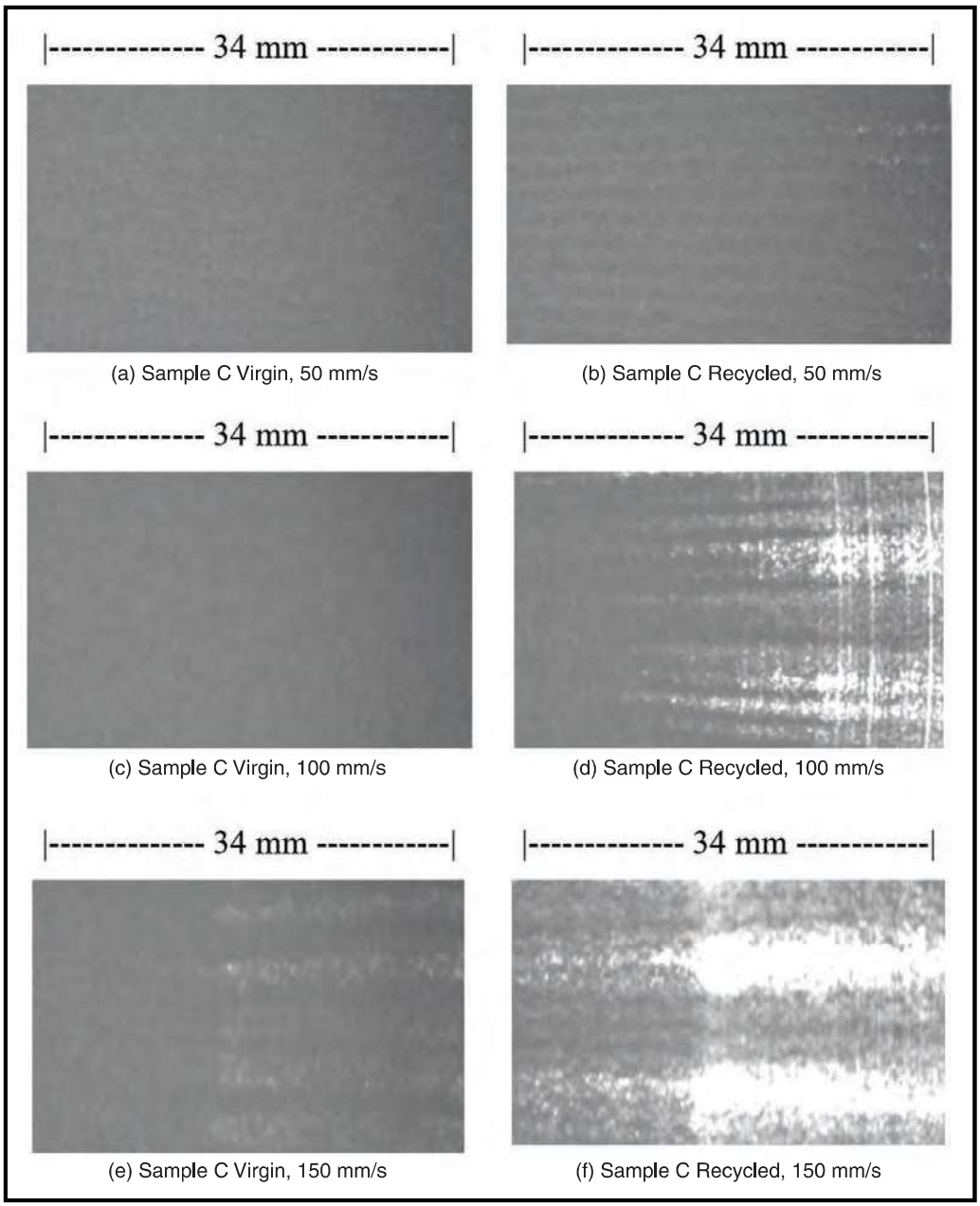

Figure 7. *Images of various as-received C samples tested with a flat-edged spreading plate, a 150 µm spreader gap, and multiple spreader speeds*

TABLE VIII. RANKING OF THE SPREADABILITY DATA FOR AS-RECEIVED A AND B SAMPLES TESTED WITH A ROUND-EDGED SPREADING PLATE, A SPREADING GAP OF 150 µm, AND A SPREADING SPEED OF 50 mm/s

Sample (as-received)	Spread Eff. %	Layer Density g/cm^3	Spread Rate mg/cm	Spread Rate SD mg/cm	Spread Unif. %	Fractal Dim.
A Recycled	52.7	4.22	220	11	0.3	2.48
A Virgin	52.5	4.20	207	13	7.2	2.63
B Virgin	44.0	3.52	184	11	1.8	3.25
B Recycled	42.9	3.43	179	12	-0.7	3.49

TABLE IX. RANKING OF THE FLOWABILITY OF HUMIDITY EXPOSED A AND B SAMPLES RANKED BY AVALANCHE ANGLE

Sample	Avalanche Energy mJ/kg	Avalanche Angle deg	Cohesion-T Pa	Dynamic Density g/cm^3	Volume Fraction
A Virgin Humid	9.9	31.6	30.0	4.67	0.57
B Recycled Humid	17.7	37.6	81.3	4.25	0.53
A Recycled Humid	19.7	46.3	97.0	4.23	0.53
B Virgin Humid	28.0	52.8	165.2	3.98	0.50

TABLE X. RANKING OF THE SPREADABILITY OF HUMIDITY EXPOSED A AND B SAMPLES TESTED WITH A FLAT-EDGED SPREADING PLATE, A SPREADING GAP OF 150 µm, AND A SPREADING RATE OF 50 mm/s

Sample	Spread Eff. %	Layer Density g/cm^3	Spread Rate mg/cm	Spread Rate SD mg/cm	Spread Unif. %	Fractal Dim.
A Virgin Humid	48.0	3.83	200	16	13.9	3.27
A Recycled Humid	40.4	3.23	170	10	-11.5	3.55
B Recycled Humid	36.2	2.89	152	8	-8.5	4.43
B Virgin Humid	5.8	0.46	27	21	-89.7	11

TABLE XI. SUMMARY OF THE SAMPLE B VIRGIN, HUMIDITY EXPOSED SPREADABILITY DATA

Sample	Spread Eff. %	Layer Density g/cm^3	Spread Rate mg/cm	Spread Rate SD mg/cm	Spread Unif. %	Fractal Dim.
B Virgin (as-received) 150 µm Gap	43.9	3.51	182	15	4.9	3.06
B Virgin Humid 150 µm Gap	5.8	0.46	27	21	-89.7	11.0
B Virgin Humid 200 µm Gap	54.1	4.33	301	32	-8.8	2.60

where it would no longer spread but would still flow.

Because the virgin B sample stopped spreading with exposure to humidity, the spreading gap was increased to 200 µm and the sample started spreading again as shown in Table XI. This is interesting because a machine will keep trying to spread another layer even if powder wasn't spread in the previous layer. In this case, if the virgin B sample was not spread in one layer, the next layer would have a larger gap where it would start spreading again. This behavior cannot be inferred from flowability data.

Spreadability and Flow of Oven Dried Samples

The flowability and spreadability of the dried A and B samples with a gap of 150 µm are presented in Table XII and Table XIII respectively. When the samples were dried after humidity exposure, the flowability and spreadability rankings changed again. In all samples, except the virgin A sample, drying improved the flow properties of the powders. After drying, most of the samples improved their spreadability but not to the levels of the as-received samples. The virgin B sample stopped spreading immediately after drying, then had

TABLE XII. RANKING OF FLOW PROPERTIES OF DRIED SAMPLES

Sample	Avalanche Energy mJ/kg	Avalanche Angle deg	Cohesion-T Pa	Dynamic Density g/cm^3	Volume Fraction
A Virgin	9.9	31.6	30.0	4.67	0.58
A Recycled	13.0	34.3	35.3	4.38	0.55
B Recycled	14.5	36.1	35.3	4.18	0.52
B Virgin	13.3	41.7	60.2	4.05	0.51

TABLE XIII. RANKING OF THE SPREADABILITY OF DRIED A AND B SAMPLES TESTED WITH A FLAT-EDGED SPREADING PLATE, A SPREADING GAP OF 150 µm, AND A SPREADING RATE OF 50 mm/s

Sample	Spread Eff. %	Layer Density g/cm^3	Spread Rate mg/cm	Spread Rate SD mg/cm	Spread Unif. %	Fractal Dim.
A Recycled Dried	45.4	3.63	191	11	-7.4	3.16
A Virgin Dried	42.1	3.37	177	8	-0.3	3.25
B Recycled Dried	42.0	3.36	177	12	-8.6	3.12
B Virgin Dried	23.1	1.84	99	25	-61	6.76

poor spreadability after a second test. The tested powder was then sealed in a container and tested again after 5 hours and then again after 16 hours and the spreadability improved a great deal. These data are presented in Table XIV. This change in spreadability appeared to be due to static charge build-up on the sample powder. This could have been the result of powder flow testing that was performed on all the samples prior to spreadability testing. This could explain why all the dried samples had poorer spreadability than the as-received samples. Presumably the as-received samples contained more moisture than the dried samples, and this could have helped mitigate static charge build-up after flow testing.

The virgin A sample had the best flowability, but the recycled A sample had the best spreadability. The virgin B sample had the poorest flowability and the poorest spreadability.

Spreadability and Flow of Segregation Stress Exposed Samples

A and B samples were subjected to segregation pressure by flowing them through multiple core-flow funnels and by pan sifting.

A summary of the flowability data for the funnel segregation test data made on the individual samples is given in Table XV. A summary of the spreadability data is given in Table XVI. The flowability of the samples did not change a great deal when exposed to segregation stress using multiple core-flow funnels. The virgin B sample displayed the most change and the recycled A sample showed more change than the virgin A sample. The virgin B sample and the recycled A sample showed lower spreadability after the funnel flow while the virgin A sample and the recycled B sample showed a small improvement.

The pan-segregation flowability data are summarized in Table XVII and Table XIX. The pan-segregation spreadability data are in Table XVIII and Table XX. For the pan-segregation test, the virgin A sample showed a small reduction in spreadability in the lower-layer sample whereas the other samples showed a large improvement in the lower-layer powder. In pan-segregation, larger particles move to the top of the pan as illustrated in Figure 8.

The data are interesting because the spreadability improved for the sample cuts with smaller particles, but the flow got worse. It appears that the larger particles created jamming in the spreading gap that reduced the spreadability. But removing the larger particles had a negative effect on the flowability. In general, the spreadability of the virgin A sample was the least sensitive to segregation stress. Segregation potential is controlled mainly by the width of the particle-size-distribution and the flowability of the material.

Images of the lower- and upper-layer pan-segregated

TABLE XIV. SUMMARY OF THE AS IS, HUMIDITY EXPOSED, AND DRIED SPREADABILITY DATA FOR B SAMPLES TESTED WITH A FLAT-EDGED SPREADING PLATE, A SPREADING GAP OF 150 µm, AND A SPREADING RATE OF 50 mm/s

Sample	Spread Eff. %	Layer Density g/cm^3	Spread Rate mg/cm	Spread Rate SD mg/cm	Spread Unif. %	Fractal Dim.
B Virgin (as-received)	43.9	3.51	182	15	4.9	3.06
B Virgin Dried	23.1	1.84	99	25	-61	6.76
B Virgin Dried 5h	35.5	2.84	147	17	-24.5	4.52
B Virgin Dried 16h	38.1	3.05	163	32	-46.9	3.80

TABLE XV. SUMMARY OF THE FUNNEL-SEGREGATED FLOW DATA FOR SAMPLES A AND B

Sample	Avalanche Energy mJ/kg	Avalanche Angle deg	Cohesion-T Pa	Dynamic Density g/cm^3	Volume Fraction
A Virgin	6.6	31.9	16.2	4.76	0.594
A Recycled	10.2	40.1	53.4	4.37	0.545
B Recycled	10.4	39.5	43.5	4.46	0.557
B Virgin	14.5	47.5	89.8	4.20	0.525

TABLE XVI. SUMMARY OF THE SPREADABILITY DATA FOR FUNNEL-SEGREGATED SAMPLES A AND B TESTED WITH A FLAT-EDGED SPREADING PLATE, A SPREADING GAP OF 150 µm, AND A SPREADING RATE OF 50 mm/s

Sample	Spread Eff. %	Layer Density g/cm^3	Spread Rate mg/cm	Spread Rate SD mg/cm	Spread Unif. %	Fractal Dim.
B Recycled	52.4	4.19	214	34	6.3	2.98
A Virgin	50.7	4.06	212	14	8.7	2.97
A Recycled	44.5	3.56	187	7	-1.5	2.95
B Virgin	35.2	2.82	148	40	2.0	8.27

TABLE XVII. SUMMARY OF THE UPPER LAYER OF PAN-SEGREGATION DATA FOR SAMPLES A AND B

Sample	Avalanche Energy mJ/kg	Avalanche Angle deg	Cohesion-T Pa	Dynamic Density g/cm^3	Volume Fraction
A Virgin	6.7	32.8	18.7	4.64	0.580
B Recycled	6.6	36.5	31.1	4.27	0.533
A Recycled	8.6	36.9	40.1	4.40	0.550
B Virgin	14.9	47.4	80.7	4.09	0.511

TABLE XVIII. SUMMARY OF THE SPREADABILITY DATA FOR UPPER LAYER OF PAN-SEGREGATED SAMPLES A AND B TESTED WITH A FLAT-EDGED SPREADING PLATE, A SPREADING GAP OF 150 µm, AND A SPREADING RATE OF 50 mm/s

Sample	Spread Eff. %	Layer Density g/cm^3	Spread Rate mg/cm	Spread Rate SD mg/cm	Spread Unif. %	Fractal Dim.
A Virgin	45.7	3.65	191	9	+7.7	3.26
A Recycled	38.1	3.05	159	19	-24.6	3.75
B Recycled	35.0	2.80	144	18	-22.7	4.39
B Virgin	27.4	2.19	119	22	-42.3	5.4

TABLE XIX. SUMMARY OF THE LOWER-LAYER PAN-SEGREGATED FLOWABILITY DATA FOR SAMPLES A AND B

Sample	Avalanche Energy mJ/kg	Avalanche Angle deg	Cohesion-T Pa	Dynamic Density g/cm^3	Volume Fraction
A Virgin	7.2	32.7	19.1	4.68	0.585
B Recycled	7.7	36.5	37.8	4.30	0.537
A Recycled	7.8	36.1	34.8	4.27	0.534
B Virgin	14.7	47.4	80.6	4.09	0.511

TABLE XX. SUMMARY OF THE SPREADABILITY DATA FOR LOWER-LAYER PAN-SEGREGATED SAMPLES A AND B TESTED WITH A FLAT-EDGED SPREADING PLATE, A SPREADING GAP OF 150 µm, AND A SPREADING RATE OF 50 mm/s

Sample	Spread Eff. %	Layer Density g/cm^3	Spread Rate mg/cm	Spread Rate SD mg/cm	Spread Unif. %	Fractal Dim.
A Recycled	53.7	4.30	224	11	-5.4	2.23
A Virgin	44.5	3.56	187	8	3.3	2.99
B Recycled	41.4	3.32	174	11	3.1	3.56
B Virgin	34.3	2.75	148	33	-54.1	4.00

test portions for Sample A in Table XVIII and Table XX are presented in Figure 9. The layer created with the upper-layer material for the recycled sample contains continuous channels in the bed surface.

Figure 8. Image of the segregation pan top surface for Sample B Recycled after sifting. Larger particles can be seen on the top surface

SUMMARY AND CONCLUSIONS

The spreadability and flowability of several AM powders have been tested using the SpreadStation Powder Spreadability Analyzer and the Revolution Powder Analyzer. The results indicate that flowability and spreadability are different measurements and have different sensitivities. Powder flow measurements quantify the interactions between particles in a powder. Spreadability measurements quantify how a powder interacts with machine hardware and machine settings. The data show some general correlations between flowability and spreadability but also specific areas where they diverge. A powder that flows well may not spread well or even spread at all, and a powder that spreads well may not flow well. An example revealed by the data concerns large and small particles in a powder mass. Increasing the number of large particles in the sample improved the flowability but reduced spreadability. Increasing the number of small particles in low concentrations reduced the flowability but improved spreadability.

The data also show that the spreadability, as mea-

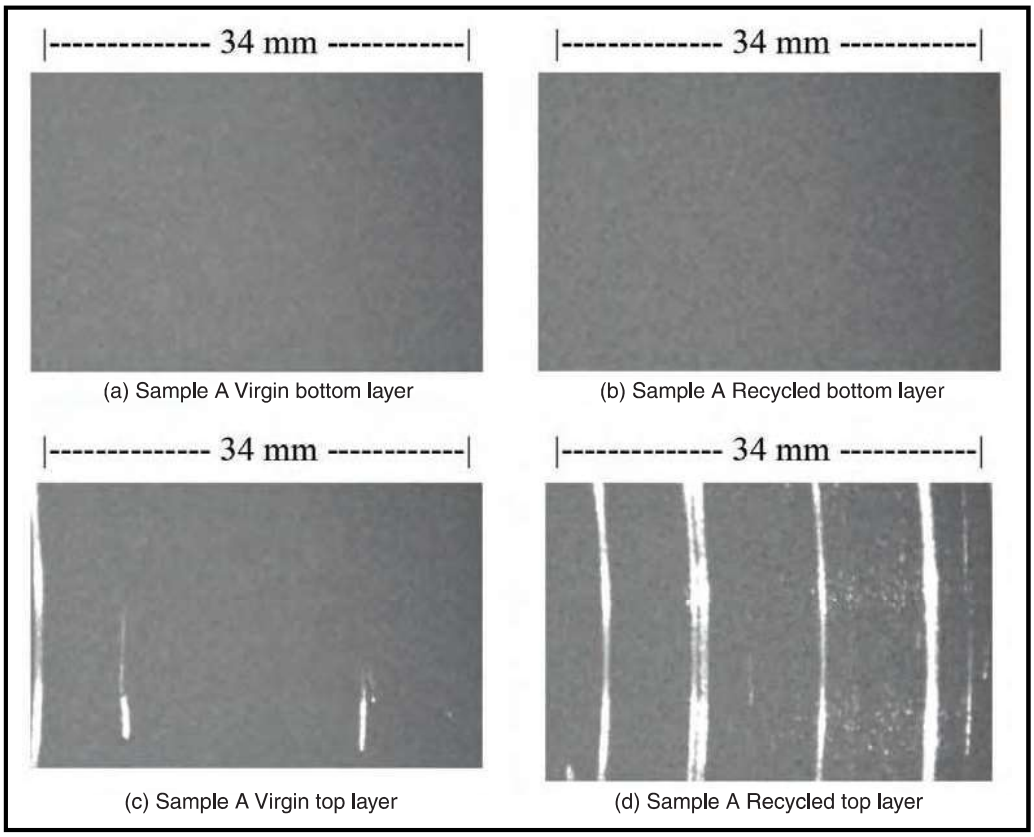

Figure 9. *Images of Sample A pan-segregated samples tested with a flat-edged spreading plate, a spreading gap of 150 µm, and a spreading rate of 50 mm/s*

sured by the instrument, changed as the spreading variables were changed, and that some materials were more sensitive to spreading variables than others. In addition, recycling powders, exposing them to humidity, drying powders, and subjecting them to segregation stress changed their spreadability and flowability, and the relationship between flowability and spreadability.

Powder flowability measurements are useful for characterizing materials, studying lot-to-lot and formula variations in powders, quantifying the effects of recycling, handling, and environmental conditions on powder flow, and analyzing powder feeding issues. Powder spreadability measurements are useful for determining if and how well a powder will spread, quantifying the effects of spreading speed, leveling height, spreader geometry, build surface and powder feeder design, and quantifying the effects of recycling, handling ,and environmental conditions in the machine on spreadability.

REFERENCES

1. C.N. Hulme-Smith, Vv Hari and P. Mellin, "Spreadability Testing of Powder for Additive Manufacturing," *BHM Berg- und Hüttenmännische Monatshefte,* 2021, vol. 166, pp.9–13.
2. M. Ahmed, M. Pasha, W. Nan and M. Ghadiri, "A Simple Method for Assessing Powder Spreadability," *Powder Tech.,* 2020, vol. 367, pp. 671–679.
3. L. Cordova, T. Bor, M. de Smit, M. Campos and T. Tinga, "Measuring the Spreadability of Pre-treated and Moisturized Powders for Laser Powder Bed Fusion," *Addit. Manuf.,* 2020, vol. 32, https://doi.org/10.1016/j.addma.2020.101082.
4. Z. Snow, R. Martukanitz and S. Joshi, "On the Development of Powder Spreadability Metrics and Feedstock Requirements for Powder Bed Fusion Additive Manufacturing," *Addit. Manuf.*, 2019, vol. 28, pp. 78–86.
5. M.Z. Gao, B. Ludwig, T.A. Palmer, Impact ofatomization gas on characteristics of austenitic stainless steel powder feedstocks for additive manufacturing, Powder Technol. In press (2020). https://doi.org/10.1016/j.powtec.2020.12.005.
6. A.T. Sutton, C.S. Kriewall, S. Karnati, M.C. Leu, J.W. Newkirk, Characterization of AISI 304L stainless steel powder recycled in the laser powder-bed fusion process, *Addit. Manuf.* 32 (2020) 100981. https://doi.org/10.1016/j.addma.2019.100981.
7. G. Martiska, "Evaluating the Spreadability of Metal Powders for Additive Manufacturing Applications Using a New Powder Spreadability Analyzer," *Proc. AMPM2021,* Metal Powder Industries Federation, Princeton, NJ, 2021.
8. G. Martiska, "Evaluating the Changing Sensitivity of AM Powders to Segregation and Humidity as They are Used and Recycled," *Proc. AMPM2021,* Metal Powder Industries Federation, Princeton, NJ, 2021.
9. T. Thornton, "Particle Size and Shape Evaluation of SS-316L Powders from Interlaboratory Study," *IJPM*, 2020, vol. 56, no. 4, pp. 41–57.
10. J.G Saad and T. Thornton, "Understanding Surface Area Measurement Techniques for Improved Powder Production," *Proc. AMPM2018,* Metal Powder Industries Federation, Princeton, NJ, 2018.
11. Mercury Scientific, Revolution Powder Analyzer User Manual, (2010) 248.
12. Y. Mahmoodkhani, U. Ali, S.I. Shahabad, A.R. Kasinathan, R. Esmaeilizadeh, A. Keshavarzkermani, E. Marzbanrad and E. Toyserkani , "On the Measurement of Effective Powder Layer Thickness in Laser Powder-Bed Fusion Additive Manufacturing of Metals," *Prog. Addit. Manuf.,* 2019, vol. 4, no. 2, pp. 109–116.
13. T. M. Wischeropp, C. Emmelmann, M. Brandt and A. Pateras, "Measurement of Actual Powder Layer Height and Packing Density in a Single Layer in Selective Laser Melting," *Addit. Manuf.,* 2019, vol. 28, pp. 176–183, https://doi.org/10.1016/j.addma.2019.04.019. ijpm